THE EFFECT OF WING SWEEP ON THE FLOW AROUND A SLAT AND ITS PERFORMANCE

by
B. Djatmiko
I.G.N. Sudira
Indonesian Aerospace Industries (IPTN)
Bandung, Indonesia

A. Cakrawala
Indonesia Low Speed Tunnel
Serpong, Indonesia

B. van den Berg
National Aerospace Laboratory NLR
Amsterdam, The Netherlands

S.H. Chintamani and M.D. Mack
Boeing Commercial Airplane Group
Seattle, Washington

Abstract. This paper discusses the results of a cooperative experimental research program on a half-model of a fuselage and wing with high lift devices (slat and flap) equipped with zero and 25 deg sweep capability.

Tests were made with two wing sweeps, 0 and 25 deg. The results include:

A. Basic forces and surface pressure distributions.
B. Three-dimensional confluent boundary layer measurements at two spanwise and three chordwise stations on the main wing.
C. Total pressure measurements at the slat cove.
D. Surface flow visualizations.

1. Introduction

The present work is an extension of a cooperative low-speed research program between IPTN/LAGG (Indonesia), NLR (Netherlands), and Boeing (U.S.A) on the effect of wing sweep on the performance of high-lift devices.

The first series of wind tunnel tests on a half-model of a fuselage and wing, executed a few years ago, produced some unexpected results at maximum lift conditions of the unswept configuration. In addition, significant non-repeatability and hysteresis problems were also encountered during the measurements. To remedy the early wing root stall of the unswept configuration, a detailed numerical study, using a panel method, was performed by IPTN engineers, with the assistance of NLR personnel [1]. It appeared from this study that the unfavourable effect of the fuselage on the flow near the wing root could be significantly reduced by changing the circular fuselage shape to a nearly square cross-section in the vicinity of the wing. Also constructional improvements were applied, notably a more aerodynamically-clean routing of the pressure tubes from the slat to the fuselage and a redesign of the slat and flap brackets to minimize the disturbance to the flow.

With the above modifications, the scope of the present tests were enhanced to include the effects of sweep on the slat wake and boundary layer and development on the main wing with optimized slat and flap. Velocity and cross-flow profiles were measured at six stations on the swept and unswept configuration.

2. Wind tunnel tests

The tests were conducted in the 3 x 4 m test section of the Indonesian Low Speed Tunnel ILST at Serpong near Jakarta. The single return, atmospheric, low speed tunnel has excellent flow quality with low turbulence. The tests were carried out on a half-model of a fuselage and a simple constant-chord, untwisted wing, which can be set at zero and 25 deg sweep angle. The model was installed on the external wind tunnel balance for measuring the total forces.

For the unswept configuration the test conditions were $M = 0.20$ at $R = 2.9. * 10^6$ based on the basic wing chord ($c = 610$ mm). According to simple sweep theory, to obtain comparable compressibility effects, the free stream Mach number for the swept configuration should be a factor $1/\cos\Lambda$ higher, which yields $M = 0.22$. The corresponding Reynolds number becomes, when taking also into account the increased basic chord

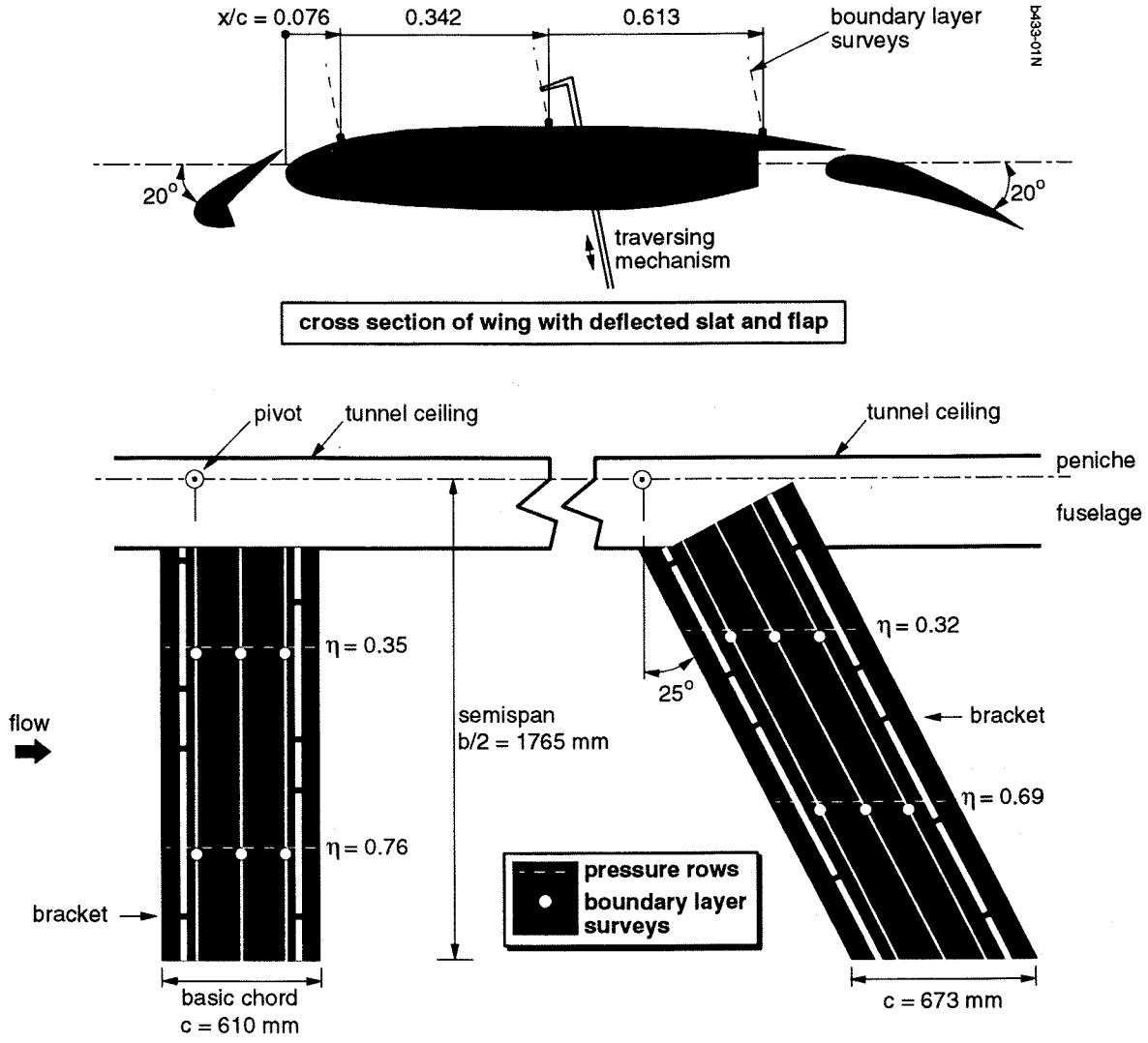

Fig. 1 Sketch of the model with the position of the measurement stations

of the swept wing (c = 673 mm), R = 3.5 * 10^6.

A typical take-off configuration was selected with 20 deg slat and 20 deg flap deflections. This choice was made to focus the research at this stage to relatively simple flows, with no large separation regions present above the flap of the swept and unswept wing.

A sketch of the model is shown in figure 1. The model is equipped with surface pressure taps at two spanwise planes for both the swept and unswept configuration. Boundary layer and wake surveys with a pressure probe were made at three inboard and three outboard stations, in the spanwise vicinity of the surface pressure measurement planes, as shown in the figure. The local static pressure at each measurement station was selected from the nearest surface pressure port.

All surveys were made on the main wing upper surface with a traverse mechanism provided by Boeing. The traversing mechanism is located on the wing lower surface side, as sketched in figure 2, inside a streamline body. The body is propelled along a post attached to the model lower surface. The post has been mounted here at a preset angle of 10 deg in order to position the streamline body better in the local flow direction at the angles of attack of interest. The probe shaft extends through the model and is well sealed to avoid any leakage. A photograph of the model with traversing mechanism is shown in figure 3. Surface pressure distributions for each configuration were measured with and without the traverse mechanism. The effect of traverse and support on the pressure distribution will be discussed later.

Principal instrumentation for the total pressure and crossflow angle measurement was a Cobra probe existing of three tubes of 0.7 mm outer diameter, see figure 2. The chamfered outer tubes and central tube were glued with epoxy. The probe was built at NLR and calibrated at various flow velocities, at pitch angles in the range +/- 10 deg and crossflow angles between +/- 30 deg. In the range of crossflow angles of ± 20 deg, using a simple calibration curve, the velocity accuracy is within

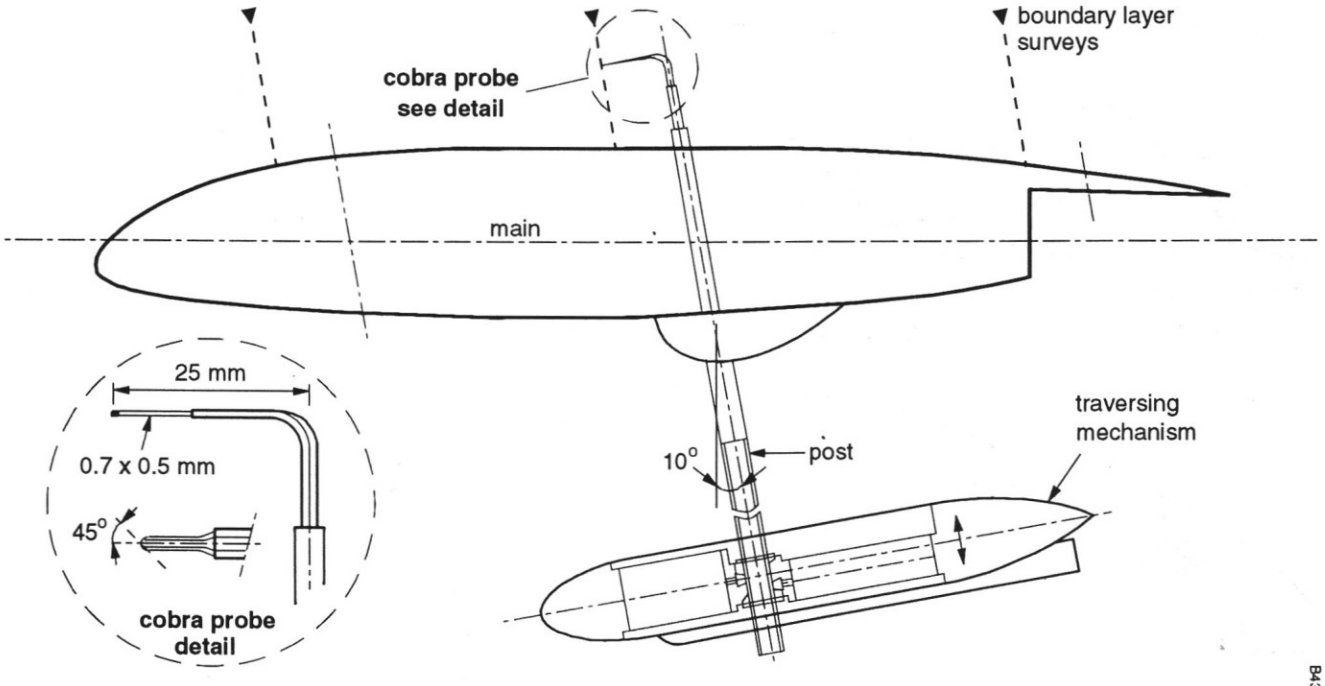

Fig. 2 Sketch of the mechanical traverse and the boundary layer probe

1 percent. The error in the measured crossflow angle is estimated to be less than 1 or 2 deg. The probe was globally oriented in the flow direction and consequently in some cases not positioned normal to the wing leading edge. In these cases the star- and backboard tube of the Cobra probe were not at equal distances from the wing surface, so that an extra error in the flow angle measurements occurs due to the velocity gradient normal to the surface. However, this error was estimated to be less than 0.5 deg.

In addition to shear flow and boundary layer surveys, a fixed total pressure rake was employed in some tests to obtain total pressure profiles in the slat cove region. Six total pressure tubes were positioned 15 deg inboard and five tubes 45 deg inboard, see figure 4. For flow angles between zero and 60 deg, one of the rows of tubes will be oriented sufficiently close to the local flow direction to measure the total pressure with reasonable accuracy. Measurement of total pressures were obtained at two spanwise stations at four angles of attack (8 to 18 deg) in order to study the growth/decay of the separation bubble in the slat cove.

To reduce the aerodynamic interference, new brackets were constructed for slat and flap. A sketch of the new slat bracket is shown in figure 4. Basically the bracket exits of two 6 mm diameter rods, located in a low-speed region not too close to the slot. Thus the effect on the flow between slat and main wing, where the flow direction varies significantly in case of sweep, is believed to be minimized. Moreover the spanwise position of the slat and flap brackets has been chosen so that no brackets are present near the measurement planes (Fig. 1).

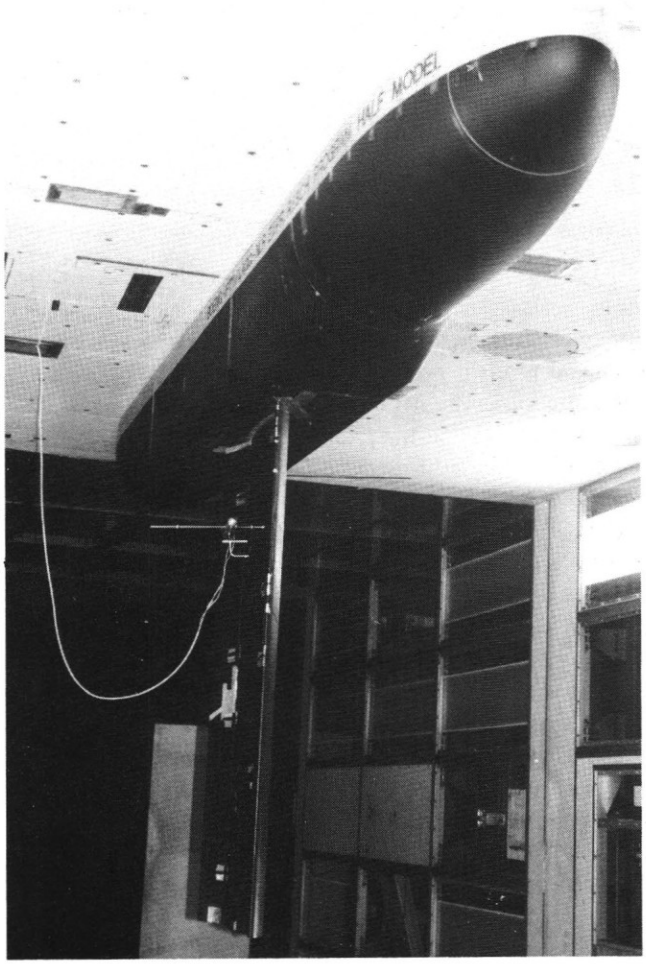

Fig. 3 High-lift half-model in the 3 x 4 m^2 test section of the Indonesian Low Speed Tunnel

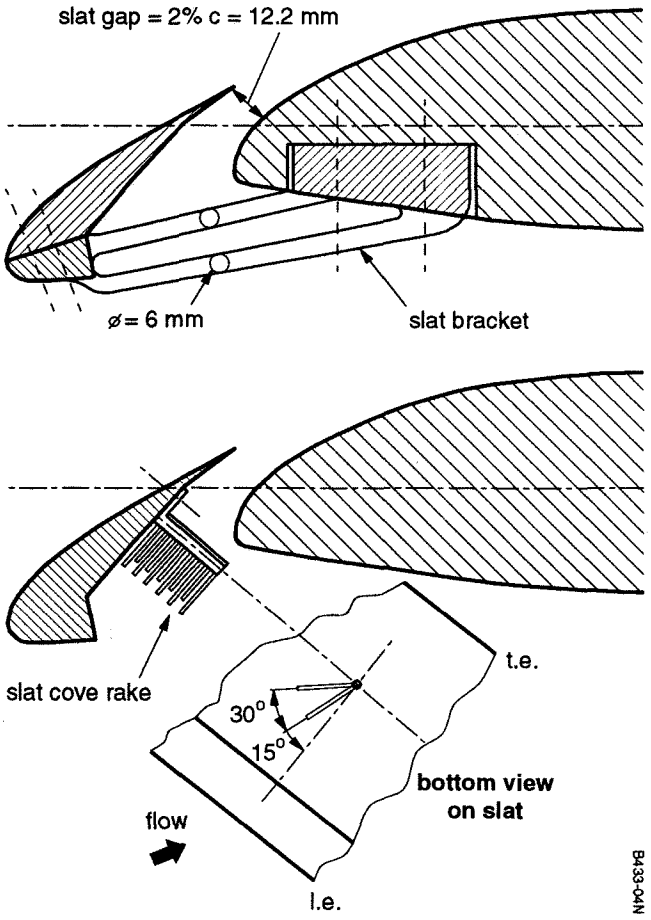

Fig. 4 Sketch of slat cove rake and slat bracket

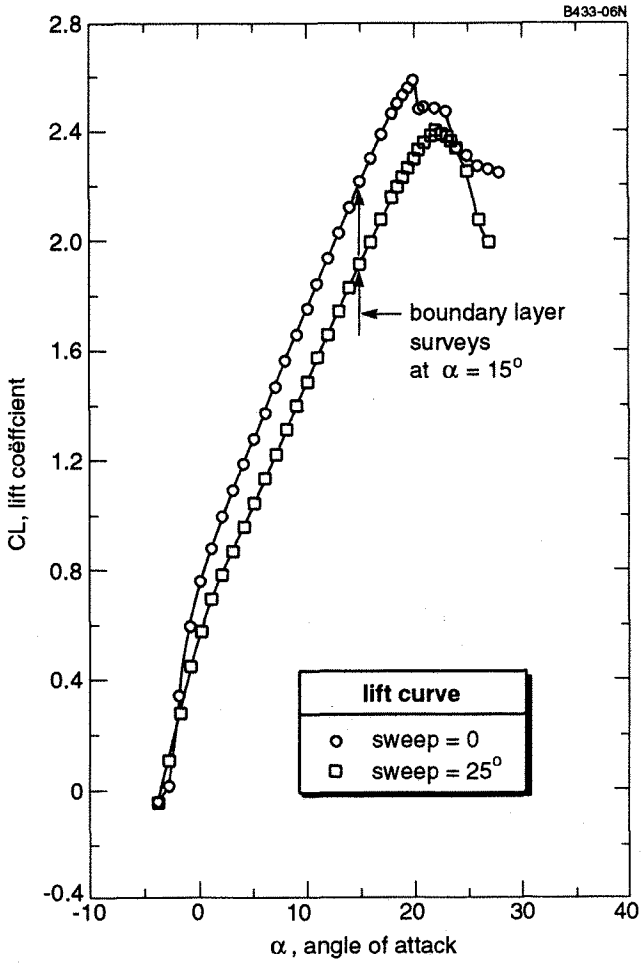

Fig. 5 Comparison of lift curves of swept and unswept configuration

3. Results and discussions

Forces. Figure 5 shows the variation of the total lift of wing and fuselage with angle of attack for the two configurations. The lift curve for the straight wing demonstrates a good linear characteristic over a substantial portion of model attitudes and has a slope of about 0.0945 per degree. The stall pattern is rather abrupt. For the swept wing the stall pattern is more gradual and the lift curve shows a substantial linear region with a slope of 0.0735 per degree, i.e. 78 % of the zero sweep value. This is fairly close to the value given by simple wing sweep theory, which predicts a factor $\cos^3\Lambda = 0.74$ for a sweep angle of $\Lambda = 25$ deg.

Also shown in figure 5 is the choice of angle of attack for the boundary layer and shear flow surveys on the main wing. At this angle of attack of 15 deg, the main wing, slat and flap are sufficiently well loaded and the flow is attached everywhere except perhaps for the flap trailing edge regions.

The variation of the drag with lift for the swept and unswept wing is shown in figure 6. The drag polars of both configurations exhibit the expected behaviour. Pitching moments were also measured but data are not included in the paper.

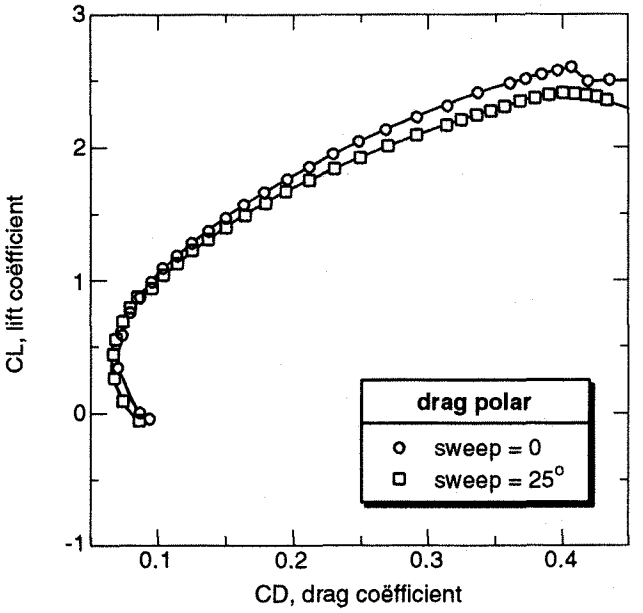

Fig. 6 Comparison of drag polars of swept and unswept configuration

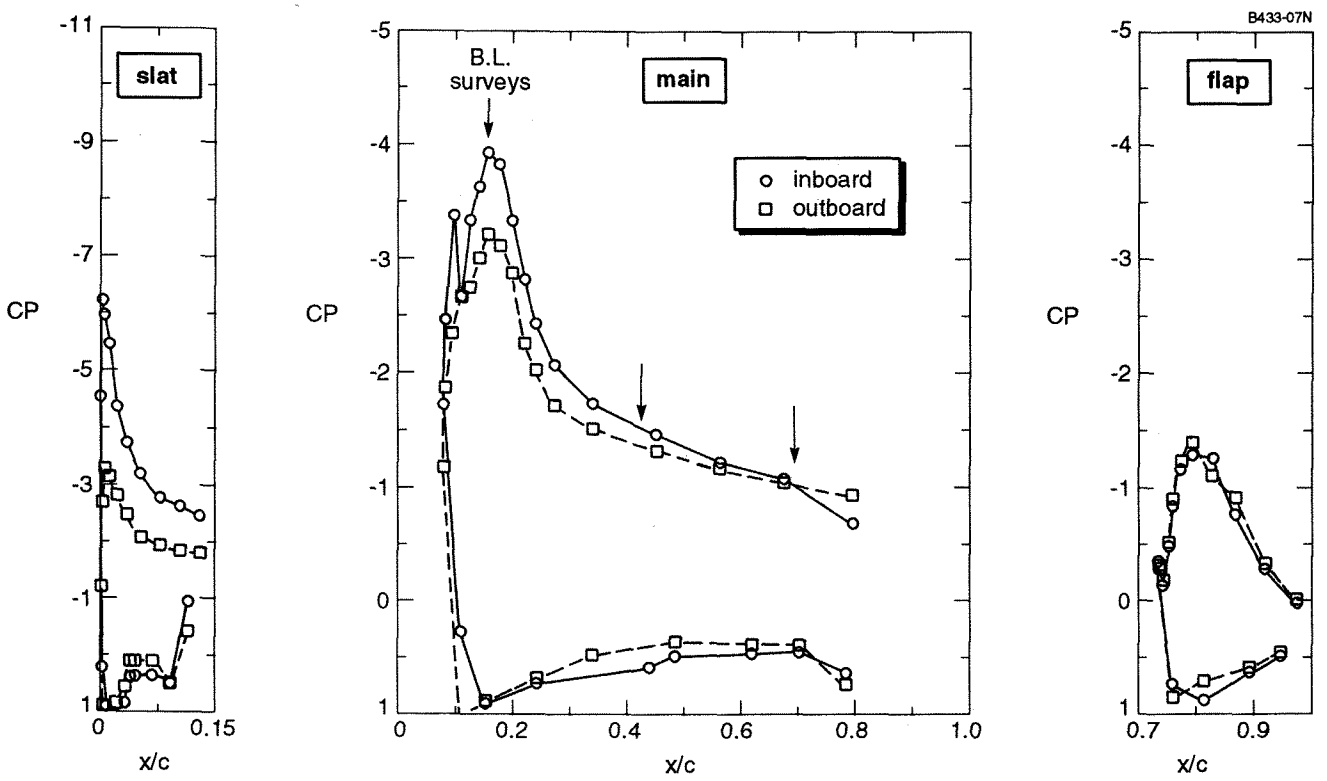

Fig. 7 Inboard and outboard pressure distributions. Sweep = 0, angle of attack15°

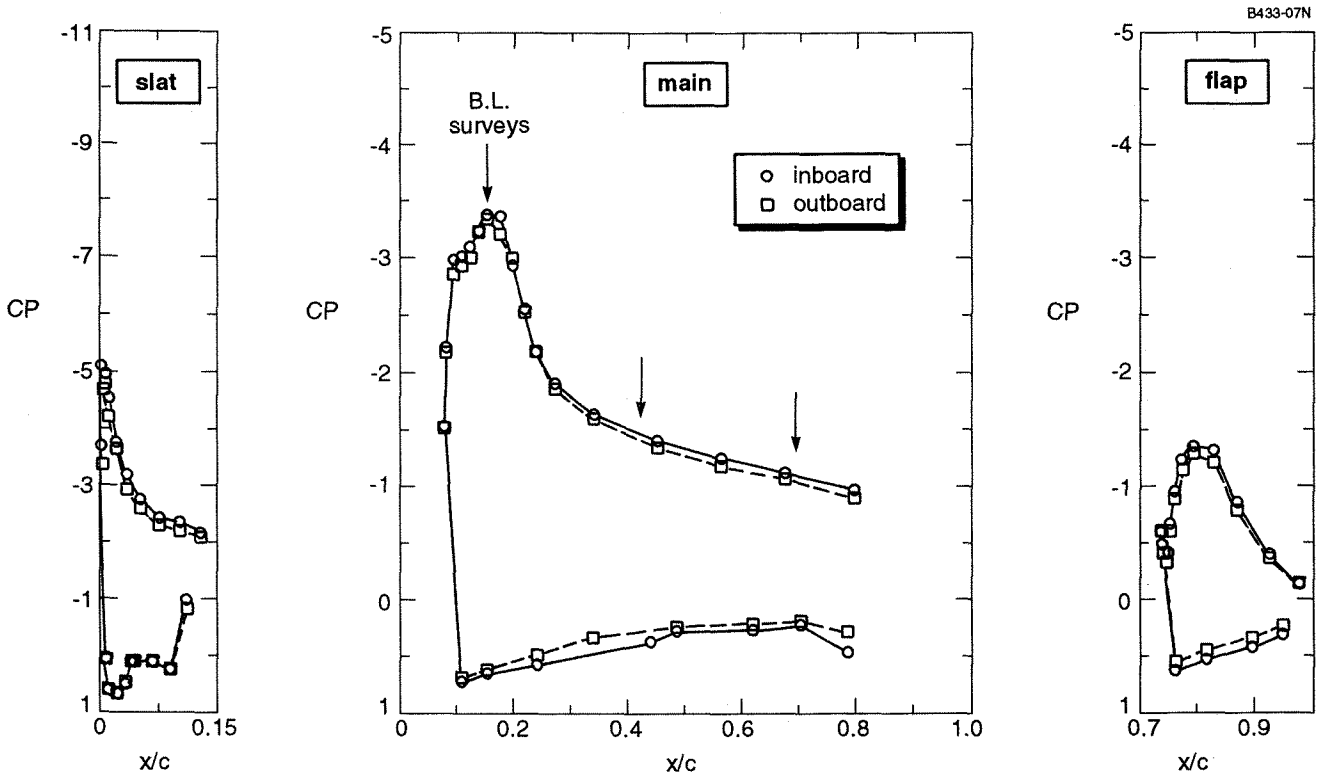

Fig. 8 Inboard and outboard pressure distributions. Sweep = 25°, angle of attack 15°

Pressure distributions. Pressure distributions on the slat, main wing and flap were obtained at several angles of attack including post stall attitudes. For the sake of discussion, the data obtained at 15 deg is shown in figures 7 and 8, for the inboard and outboard pressure measurement planes. Figure 7 shows the pressure distribution comparison for the straight wing. The loading on the slat is substantially lower outboard compared to inboard. The same trend is exhibited on the main wing, although to a lesser degree. This trend is not seen for the swept configuration, see figure 8. In this case the loading appears to be much more equal at the inboard and outboard measurement planes.

It is clear from figures 7 and 8 that the load on the slat of the straight wing is comparatively low on the outboard section. This suggests that to study the effect of sweep on the flow around the slat, it is better to focus on the inboard sections, where the slat load seems to be more similar on the swept and unswept configuration. This can be made more concrete, using simple sweep theory arguments. According to simple sweep theory, for comparable flows $C_{p,swept} = \cos^2\Lambda * C_{p,unswept} =$

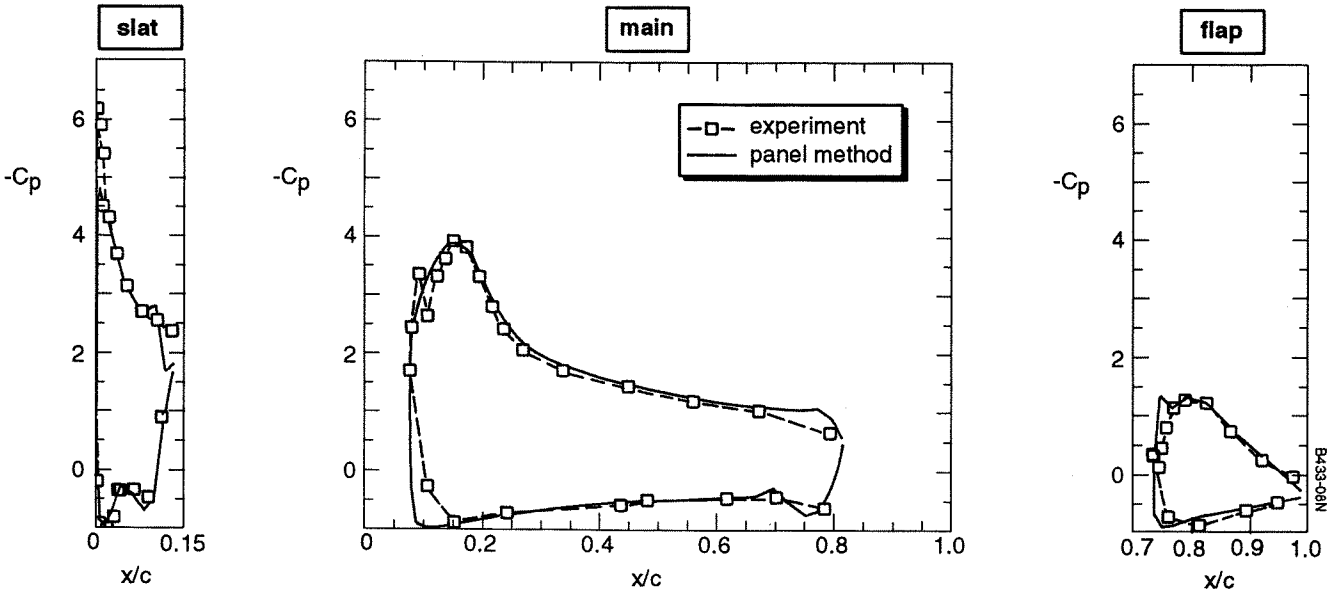

Fig. 9 Comparison of calculated and measured pressure distributions. Inboard wing section. Sweep = 0°, angle of attack = 15°

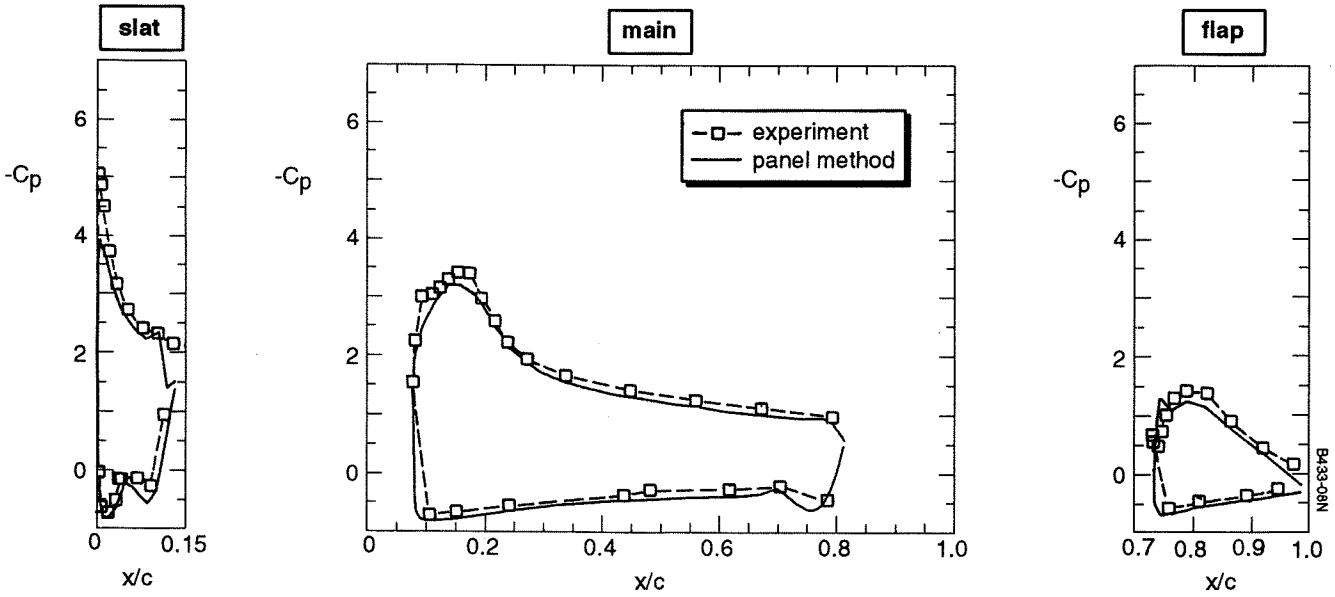

Fig. 10 Comparison of calculated and measured pressure distributions. Inboard wing section. Sweep = 25°, angle of attack = 15°

$0.82 * C_{p,unswept}$ for $\Lambda = 25$ deg. At zero sweep the inboard suction peak on the slat (Fig. 7) is $C_p = -6.2$, which yields for 25 deg sweep according to simple sweep theory $C_p = -0.82 * 6.2 = -5.1$. This value happens to be equal to the measured inboard suction peak on the swept wing (Fig. 8). On the main wing the inboard suction peak at zero sweep is $C_p = -3.95$, which yields for 25 deg sweep $C_p = -0.82 * 3.95 = -3.24$ compared to a measured value $C_p = -3.4$. It can be concluded that the conditions along the inboard measurement plane are well suited for an evaluation of the effect of sweep on the viscous flow, as will be discussed later.

In figures 9 and 10 comparisons are made with the inviscid pressure distribution, calculated with a panel method [1]. The agreement between calculation and measurement data is seen to be reasonable on the whole. The apparent underestimation of the suction pressures on the slat is not unusual for panel method calculations. At the trailing edges of the wing elements the accuracy of the calculations is in doubt. The slat and main wing cove had to be faired in a rather arbitrary manner for the calculations, so that some differences with experiment on the main wing and flap nose lower side may be expected.

In order to study the effect of the traverse mechanism on the pressure distribution, surface pressure distributions were obtained with traverse mechanism and support systems positioned on the wing lower surface at representative chordwise stations. The effect was found to be small in general. Figure 11 shows the pressure distributions with and without traverse mechanism for the straight wing. In this case the traverse position is at $x/c = 0.613$ (see Fig. 1) and inboard. For this traverse position an additional support structure for the mechanical traverse was located in the cove of the main wing. It appears from figure 11 that the pressure distribution on the main wing is slightly affected at the boundary layer traverse position. The magnitude of ΔC_p at the measurement point is of the order of 0.05. Also note that the flap pressure distribution is significantly different, with reduced suction peak and premature separation at the trailing edge. Redesign of the additional support structure necessary at this position will be considered in the next series of tests.

Slat cove flow. Total pressure measurement results from the rake at the slat cove for the swept case are shown in figure 12 at various angles of attack from 8 through 18 deg. The results from both rakes, which have a different orientation (see also Fig. 4), are plotted. The dashed lines represent plausible distributions, based on the assumption that the higher data are most likely the more accurate total pressures. The results show (qualitatively at best) that the separation bubble height in the slat cove shrinks with increasing angle of attack. Also the slat cove bubble size appears to be nearly invariant with respect to spanwise position. This indicates that the

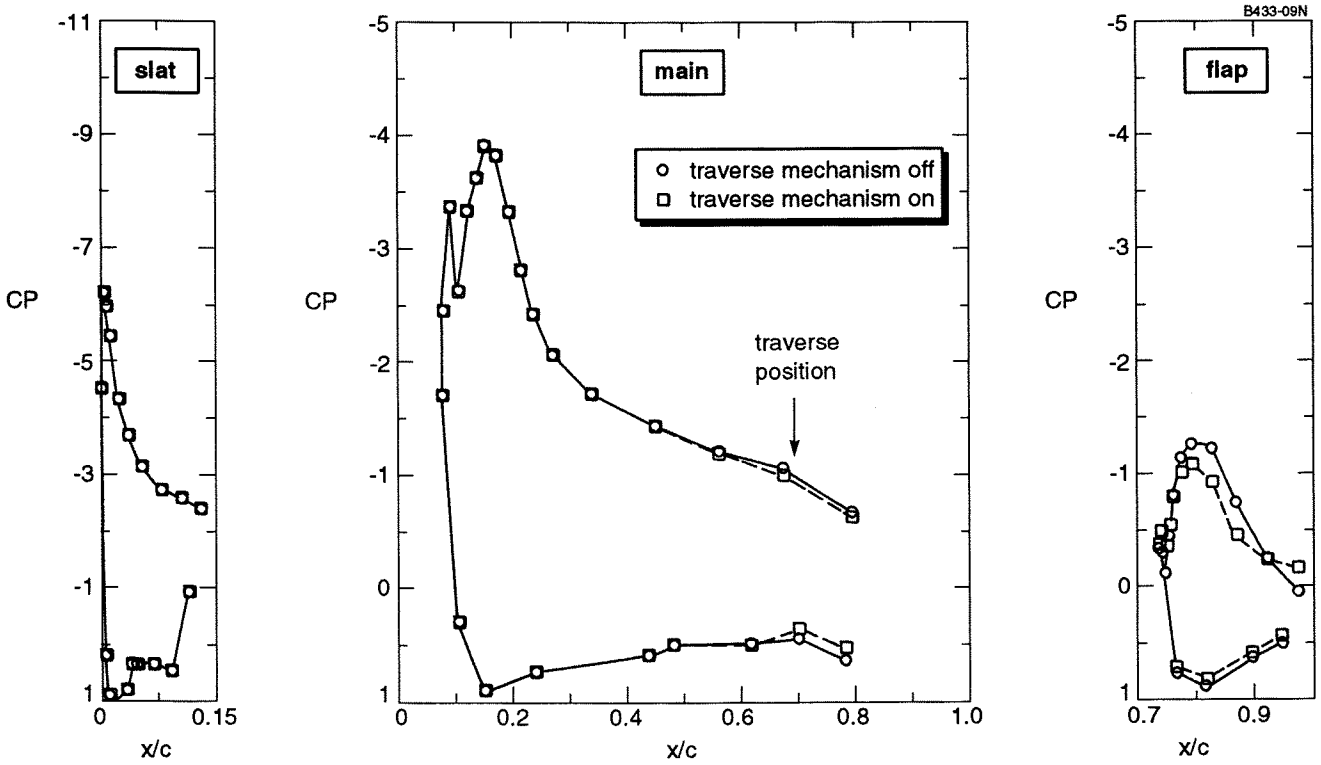

Fig. 11 Effect of traverse mechanism on inboard pressure distribution. Mechanism located rear-inboard. Sweep = 0, angle of attack = 15°

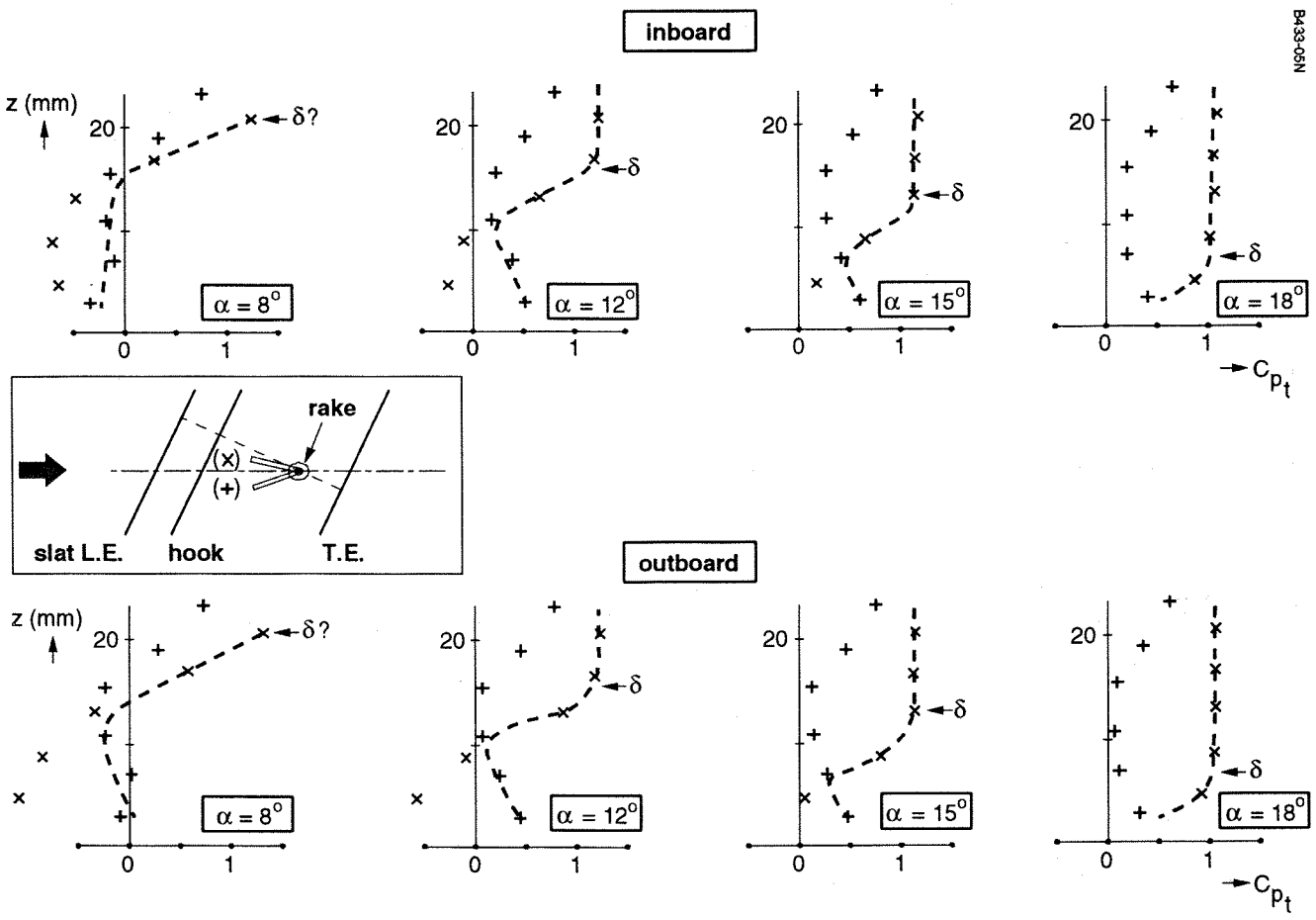

Fig. 12 Slat cove rake results at various angles of attack α. Sweep = 25°

separated flow in the slat cove is spanwise reasonably uniform. More detailed measurements with better instrumentation like hot wire/hot films are needed to draw definite conclusions.

Surface flow visualization. Sublimation tests with naphthalene and freon were conducted at 15 deg angle of attack. Visualization of natural transition showed generally clear transition patterns for both configurations. The results indicated that the natural transition location was usually near the pressure suction peaks on the wing elements, as expected.

Fluorescent oil to visualize the surface flow was utilized. The tests were made to examine local areas of separation, if any, on the modified fuselage, the wing fuselage junction and the main wing, slat and flap. The results showed orderly flow around the model, with no large separations. The visualized surface streamlines indicate the local skin friction lines. For both configurations, there was no evidence of strong spanwise flow, except in the flap trailing edge regions, where the flow is close to three-dimensional separation.

Velocity profiles. Velocity magnitudes, derived from total pressure traverses and local static pressures, have been obtained at three chordwise and two spanwise positions on the straight and swept wing. As argued earlier, the load on the wing and its elements at zero and 25 deg sweep is comparable at the inboard measurement plane, in contrast with the load outboard on the wing. Therefore the evaluation of the effect of sweep on the viscous flow has been restricted to the results at the inboard stations. The velocity profiles measured at the inboard stations are plotted in figures 13 and 14 for the straight and swept wing respectively.

At the forward stations, x/c = 0.076, the probe could not be positioned touching the surface, because of the probe being bent to a right angle (Fig. 2). Consequently velocity profiles from a height of 5 mm above surface are only available here. At these forward stations the main wing boundary layer is expected to be between 1 to 2 mm thick at most, so that measurements with a 0.7 mm thick probe anyway would not have produced reliable boundary layer data.

The slat wake is well captured as appears from the figures 13 and 14. The center of slat wake is at a height of 12 to 13 mm from the surface at the forward measurement station for both swept and unswept configurations. Slat wake development is gradual with moderate mixing, whereas the boundary layer thickness

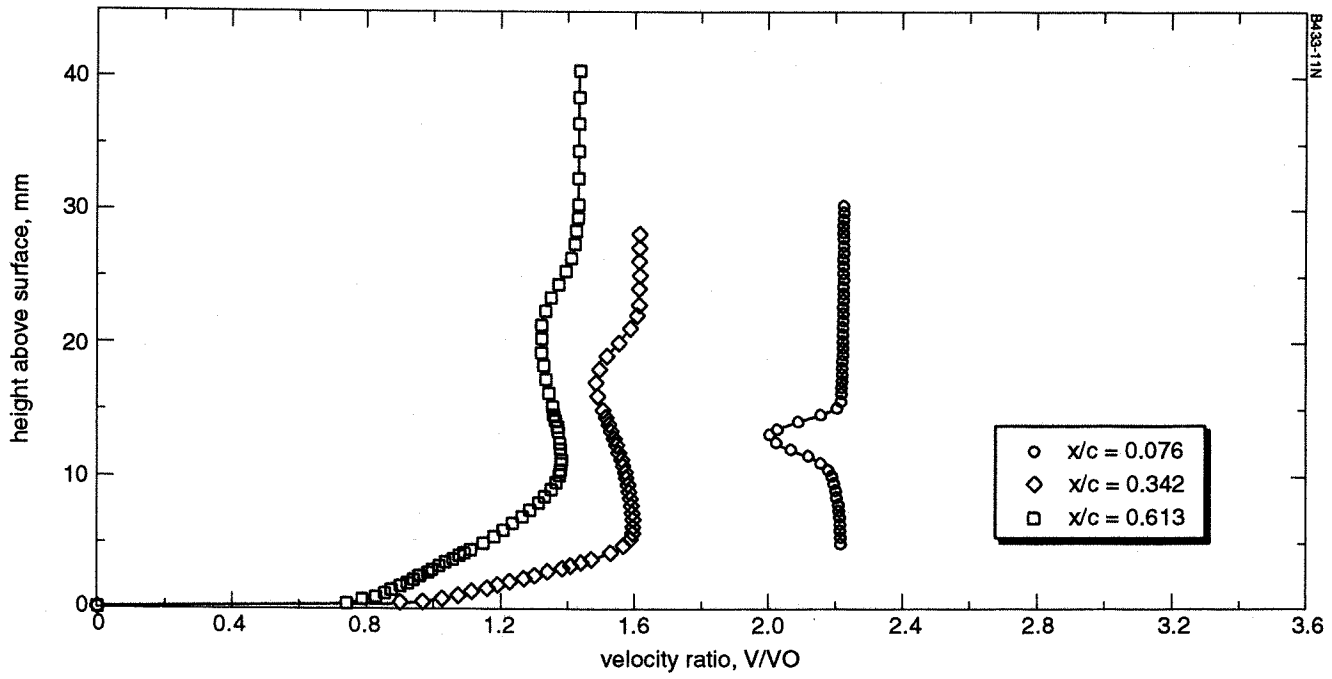

Fig. 13 Inboard velocity profiles. Sweep = 0, angle of attack = 15°

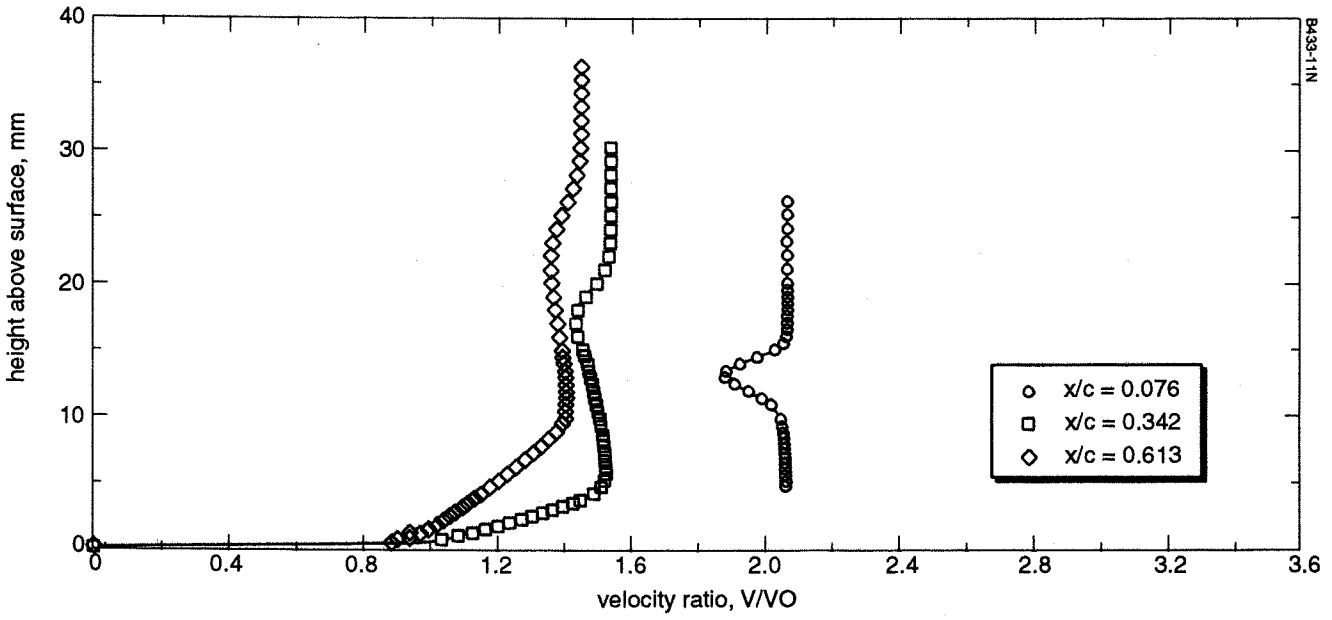

Fig. 14 Inboard velocity profiles. Sweep = 25°, angle of attack = 15°

on the main wing increases almost twice from x/c = 0.342 to 0.613. At the latter station the main wing boundary layer and the slat wake are mixed indicating complete confluence.

When comparing the velocity profiles in figures 13 and 14, it is evident that the differences between the measured profiles on the swept and straight wing are small. It appears that the development of slat wake and wing boundary layer are very similar here with and without sweep. The general conclusion to be drawn from the measurements, carried out up to now, must be that the effect of a sweep of 25 deg on the viscous flow around the slat and the downstream flow above the main wing is very moderate. Further measurements will be executed in the future to investigate whether this conclusion still holds at other angles of attack, notably angles closer to stall.

Crossflow angle profiles. Again the discussion will be restricted to the experimental data obtained inboard, as the local load on the swept and unswept configuration are better comparable there. The flow angle variation measured at the three inboard chordwise positions on the swept wing is plotted in figure 15. Positive angles indicate a flow in outboard direction.

The figure includes one curve representing the measured distribution at zero sweep at the most rearward station. It is evident that on the straight wing at this inboard station the flow is nearly collateral. The angle variation is about 2 deg, being just more than the estimated measurement error band. The angle in the outer potential flow is very close to zero, i.e. the outer flow is nearly chordwise here.

Also in case of sweep the crossflow angles are not very large. At the most rearward position, x/c = 0.613, the total flow angle variation measured across the wing boundary layer and the slat wake is no more than approximately 5 deg. The measured angle distributions at x/c = 0.342 and 0.613 show a very familiar crossflow angle profile associated with the three dimensional boundary layers on a swept wing [2, 3]. The flow in the boundary layer is directed more outboard than the outer potential flow streamlines, as one would expect. The direction of the outer potential flow varies from about 9 deg inboard at the forward station to 4 deg inboard at the rearward station.

4. Conclusions and recommendations

* The redesigned half-model of a variable sweep high-lift wing with fuselage, described in this paper, is a suitable research tool for the investigation of the effect of sweep on the flow around wings with slats and flaps and their performance.
* Total forces and moments, and surface pressure distributions at two spanwise positions, were measured over a range of angles of attack up to and beyond stall for the model at zero and 25 deg wing sweep. Detail viscous flow data at various positions behind the slat have been obtained for the swept and unswept wing at one angle of attack.
* The results of the detailed measurements in the viscous flow behind the slat above the main wing, made at 15 deg angle of attack, suggest that the effect of sweep on the viscous flow around the slat is rather more moderate than one might have expected.
* In the future further viscous flow measurements have been planned to improve understanding of the complex physics of these flows. More advanced measurement techniques at more positions on and behind the wing at more angles of attack, especially angles closer to stall, will be carried out.
* The ultimate objective of the experiment is to obtain a good and simple test case for evaluating computational methods for high-lift wings, notably to check their capability to predict the effect of sweep on the performance of the high-lift devices.

Acknowledgments

The authors sincerely acknowledge the support provided by the following key personnel of this joint research project:

* Prof. Harijono Djojodihardjo of IPTN, Indonesia
* Mr. Ronald Bengelink, Chief Engineer, Boeing Commercial Airplane Group

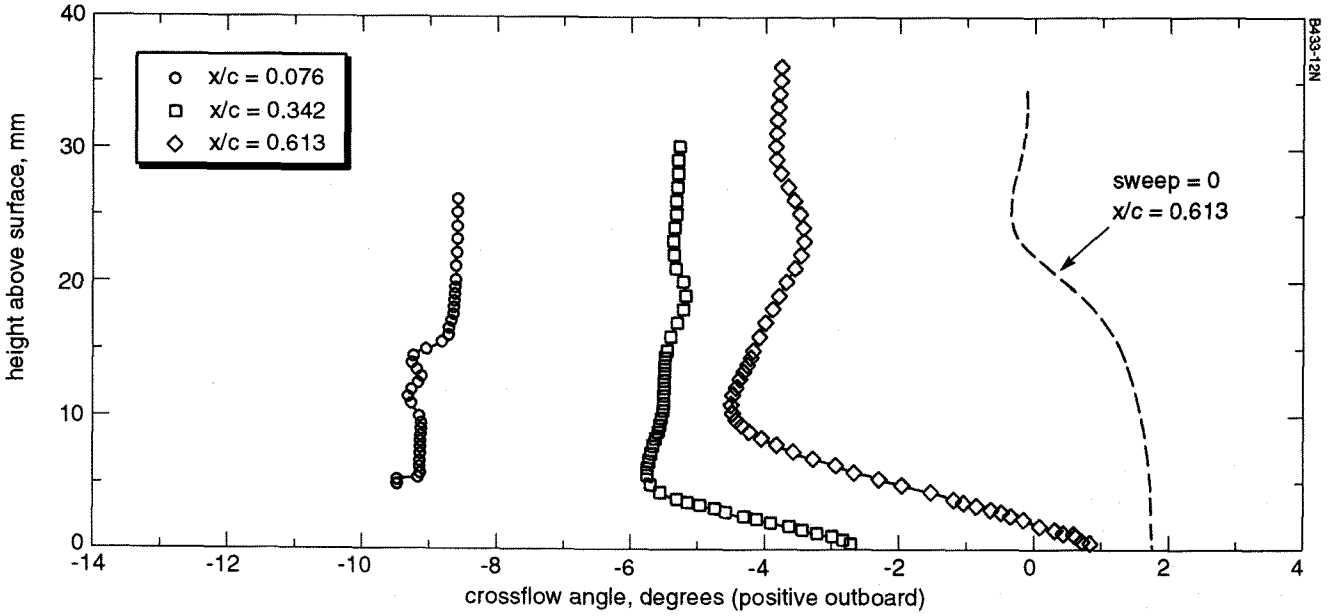

Fig. 15 Inboard crossflow angle profiles. Sweep = 25°, angle of attack = 15°

* Dr. B.M. Spee, Director of NLR, The Netherlands
* Ir. A. Adibroto and Ir. Hadidjah Modjo of LAGG, Indonesia

List of references

1. Djatmiko, B.; Sudira, IGN; Rozendal, D. - "IPTN/LAGG/Boeing/NLR cooperative research program: Aerodynamic re-design of the high lift half model". NLR TR 92418 (1992)

2. Seetharam, H.C.; Pfeifer, N.J.: Ohmura, M.; McLean, J.D. - "Experimental and theoretical studies of three-dimensional turbulent boundary layers on an empenage of a typical transport airplane". ICAS paper 82-64 (1982)

3. Berg, B. van den - "Three-dimensional shear layer experiments and their use as test cases for calculation methods". In: AGARD Report No. 741: "Computation of three-dimensional boundary layers including separation" (1987).